Correspondence

Performance of an FH Multilevel FSK for Mobile Radio in an Interference Environment

RAMÓN AGUSTÍ AND GABRIEL JUNYENT

Abstract—**This paper considers a frequency-hopped multilevel frequency shift keying (FH-MFSK) spread-spectrum communication system applied to cellular mobile radiotelephony. We present a mobile-to-base transmission model that allows us to study system impairments, such as interference from nonsynchronous users and adjacent frequency channels in the presence of matched tuned receiver filters. For intercell interference, the usual Gaussian approximation is used, but the variance calculation takes into account shadow fading. Power control in the mobiles, a mean path loss exponent of −3.5 and fast Rayleigh and slow lognormal fading have been assumed.**

We have obtained results with mobile-to-base communication of 32 kbits/s per user in a 20 MHz (one-way) bandwidth. In an isolated cell system a bit error probability less than 10^{-3} can be maintained with up to 110 simultaneous users for practical average SNR ratio of 25 dB. The presence of intercell interference degrades the bit error probability enormously, and clustering of cells is required for controlling interference.

I. INTRODUCTION

In order to provide digital mobile radiotelephony communication services to a great number of users, spread-spectrum modulation techniques using frequency-hopped (FH) frequency shift keying (FSK) have been investigated recently [1].

Assigning to each user a different tone sequence as his address, the FH-MFSK system allows many users to share the same frequency band. Because the address is spread in frequency, the system behaves well in the presence of selective fading, making it particularly suitable for mobile service in an urban environment. Nevertheless, its performance is limited by mutual interference between users.

In this paper we introduce a new model to study this interference. Our model generalizes the simplified model presented in [1]. Specifically, we analyze the mobile-to-base transmission by nonsynchronous users, tuned matched filtering at the receivers, and interchannel interference. We have also analyzed the performance of a multicell system whose service area is divided into hexagonal cells of equal size, each of them with a base station at its center. Each cell uses all the available bandwidth, which produces an intercell interference and an additional performance degradation.

Throughout our discussion, we assume the existence of a power control mechanism [2] that makes it possible for the base station to receive the same average power from each mobile assigned to it. This power control, although not strictly necessary for the system operation, would nevertheless enhance the FH-MFSK system performance by easing design constraints on the RF preamplifier and by limiting intracell interference. It may also serve to assign to each mobile the most appropriate base station for adequate reception.

The results obtained are, in general, in agreement with those in [1], and we extend them in some directions.

Paper approved by the Editor for Communication Theory of the IEEE Communications Society for publication without oral presentation. Manuscript received July 1, 1981; revised October 5, 1982.

The authors are with the Escuela Tecnica Superior de Ingenieros de Telecomunicacion de Barcelona, Universidad Politecnica de Barcelona, Barcelona 34, Spain.

II. SYSTEM DESCRIPTION

In this multiple-access modulation scheme, every T seconds, each user transmits his information in blocks of K bits. For this purpose the system has available 2^K different frequencies numbered 0, 1, ···, $2^K - 1$. With no other users, message transmission requires only one time interval of T seconds duration, and it is accomplished by the obvious assignment of messages to frequencies. With $M > 1$ simultaneous users, $L > 1$ intervals of duration $\tau = T/L$ are used, and frequency hopping is employed to allow communication in the presence of interference from other users. During the basic signaling interval T, the mth user (the subscript m denotes one link in a multiuser system) has an address generator that generates a sequence of L numbers, each K bits long:

$$V_{m,1}, V_{m,2}, \cdots, V_{m,L}.$$

Each user m is assigned a unique sequence $V_{m,l} (l = 1, \cdots, L)$ which is used to distinguish his messages from those of others. We also refer to this sequence as the address vector of user m. The transmitted tone sequence, at the rate of one tone (chip) every τ seconds, is assigned by the modulo 2^K sum ($\oplus$) of the address and the K-bit code word X_m.

$$Y_{m,l} = X_m \oplus V_{m,l}; \qquad l = 1, 2, \cdots, L.$$

At the receiver, demodulation and modulo 2^K subtraction (Θ) by $R_{m,l}$ are performed every τ seconds, yielding

$$Z_{m,l} = Y_{m,l} \ominus V_{m,l} = X_m.$$

The sequence of operations is illustrated by the matrices of Figs. 1 and 2 (see also [1]), where the 2^K tones have been placed at intervals of $1/\tau$ Hz.

Noise, multiuser interference, interchannel interference, etc., can influence the detection matrix by causing a tone to be detected when none has been transmitted (insertion). In addition, the receiver can omit a transmitted tone (miss) and cause a detection matrix to have no complete row. To allow for this possibility, we use the majority logic decision rule: choose the code word associated with the row containing the greatest number of entries (Fig. 3).

The computation of bit error probability P_B can be carried out knowing the insertion probability P_I and the miss probability P_{miss} (see [1]).

III. TRANSMISSION MODEL

A. Isolated Cell System

If we assume that the address code for each mobile is randomly generated, the probability, conditioned on the

0090-6778/83/0600-0840$01.00

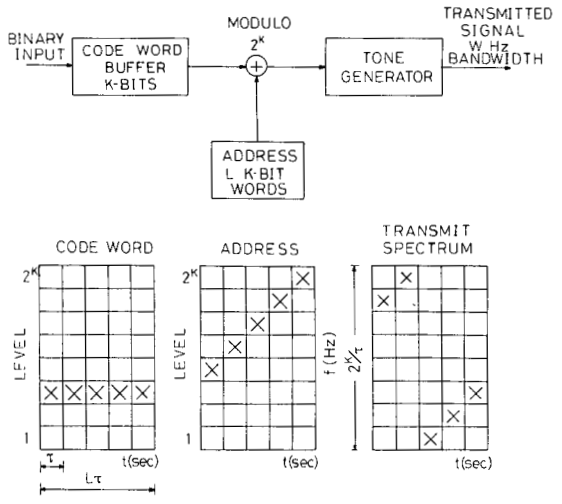

Fig. 1. Transmitter FH-MFSK.

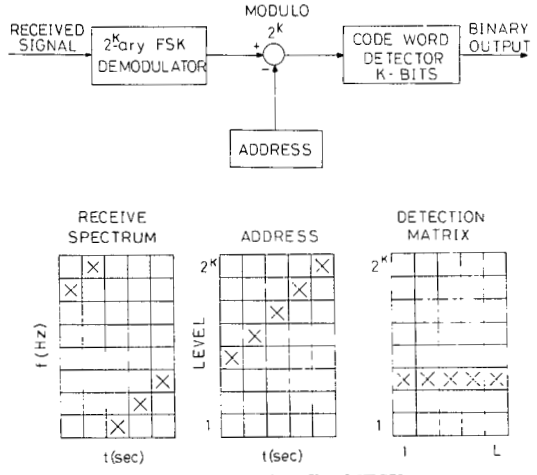

Fig. 2. Receiver FH-MFSK.

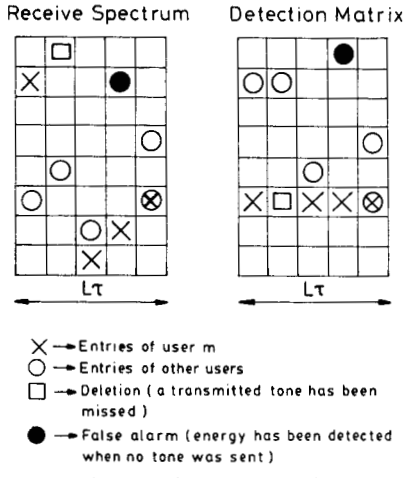

Fig. 3. Decoding matrices at the receiver of mth user.

existence of only one user, that a tone corresponding to the frequency channel j ($1 \leqslant j \leqslant 2^K$) is present in a given interval of duration τ is

$$p = \frac{1}{2^k}.$$

Consider now the presence of M nonsynchronous users transmitting simultaneously. In any interval of duration τ there are M randomly generated epochs, or time instants, coinciding with the changes in the user's chip frequency transmission. The probability that in the given interval there are N epochs in which the new chip frequency transmission corresponds to the frequency channel j is

$$P_N = \binom{M}{N} p^N (1-p)^{M-N}.$$

If $M \gg 1$ and $p \ll 1$ we can approximate the binomial distribution by a Poisson distribution [3] giving

$$P_N \cong e^{-Mp} \frac{(Mp)^N}{N!}.$$

Hence, the average number of epochs in the frequency channel j during an interval of duration τ is

$$Mp = \lambda\tau.$$

That is, we can model the multiuser interference as an uniform Poisson process of parameter

$$\lambda = \frac{M}{\tau 2^K}.$$

The above approach allows us to write the multiuser interference signal present at the receiver input in any chip interval of the desired signal as

$$z(t) = \sum_{i=-\infty}^{\infty} \sum_{j=1}^{2^K} R_{i,j} \cos\left[2\pi f_j (t - t_{i,j}) + \theta_{i,j}\right] \cdot \operatorname{rect}_\tau (t - l\tau - t_{i,j});$$

$$l\tau \leqslant t < (l-1)\tau, \quad l \text{ integer}$$

where f_j is the frequency corresponding to the frequency channel j, $R_{i,j}$ are statistically independent random variables and each is Rayleigh distributed (short-term fading), $\theta_{i,j}$ are statistically independent random variables and each is uniformly distributed over $[0, 2\pi]$,

$$\operatorname{rect}_\tau (t) = \begin{cases} 1 & 0 \leqslant t < \tau \\ 0 & \text{otherwise} \end{cases}$$

and $\{t_{i,j}\}$ is a Poisson random point process corresponding to the frequency channel j (i.e., there are 2^K Poisson processes). Moreover, $R_{i,j}$, $\theta_{i,j}$, and $\{t_{i,j}\}$ are all mutually independent. The sequence of epochs, which is due to nonsynchronous users, distinguishes this model from the base-mobile model used in [1] where the arrival times are synchronized to the beginning of the chip.

Power control is employed which maintains the mean power received by each station from mobiles in its cell to $P = \frac{1}{2}E(R_{i,j}{}^2)$. This power control eliminates the changes in signal level due to path loss variations and the effects of shadow fading.

We have also assumed that all the arrival tones in the frequency channel j fade independently of each other, because

fading tends to be caused by phenomena in the vicinity of the mobile.

The received complex envelope signal at the base station in the, say, frequency channel j (the subindex j will be omitted from now on for the sake of clarity in the notation) is

$$z_I(t) = Re^{-j\theta}\,\mathrm{rect}_\tau(t) + \sum_{i=-\infty}^{\infty} R_i e^{-j\theta i} \cdot \mathrm{rect}_\tau(t - t_i) + n(t); \qquad 0 \leqslant t < \tau.$$

The first term in the above formula corresponds to the desired signal. The second corresponds to the multiuser interference signal, and $n(t)$ is the white Gaussian noise present at the 2^K-ary FSK receiver input. This receiver sets up a tuned filter on the 2^K transmitted frequencies (see Fig. 4). Every filter is followed by an envelope detector and a threshold decision circuit.

The presence of nonsynchronous users prevents the adoption of modulation schemes with 2^K orthogonal tones, each of duration τ seconds, maintaining a bandwidth of at least $W = 2^K/\tau$ Hz as in [1].

If the frequency channel spacing adopted is the reciprocal of the chip interval, then an additional impairment appears due to adjacent channel interference (a bandwidth penalty would be needed to remove it). If we denote by $h(t)$ the complex envelope impulse response of the filter corresponding to the desired frequency channel, the complex envelope signal at the output, taking into account the interference due to the IR higher adjacent channels and the IL lower channels, is

$$z_0(t) = \underbrace{Re^{-j\theta}S_0(t)}_{1} + r(t) + n_f(t); \qquad 0 \leqslant t < \tau$$

with

$$r(t) = \underbrace{\sum_{i=-\infty}^{\infty} R_i e^{-j\theta i} S_0(t - t_i)}_{2} + \underbrace{\sum_{\substack{c=-IL \\ c\neq 0}}^{IR} \sum_{v=-\infty}^{\infty} R_{v,c} e^{-j\theta_{v,c}} S_c(t - t_{v,c})}_{3}$$

where 1) is the desired signal, 2) is the multiuser interference signal, and 3) is the adjacent channel multiuser interference signal,

$$S_c(t) = \tfrac{1}{2}\,\mathrm{rect}_\tau(t) e^{-j2\pi \frac{c}{\tau} t} * h(t); \qquad c = -IL, \cdots, 0, \cdots, IR,$$

$\{t_{v,c}\}$ is a Poisson random point process corresponding to the cth adjacent frequency channel, $R_{v,c}$ and $\theta_{v,c}$ are identically distributed random variables as the $R_{i,j}$ and $\theta_{i,j}$ previously mentioned, and

$$n_f(t) = \tfrac{1}{2}\, n(t) * h(t) = n_x(t) + j n_y(t).$$

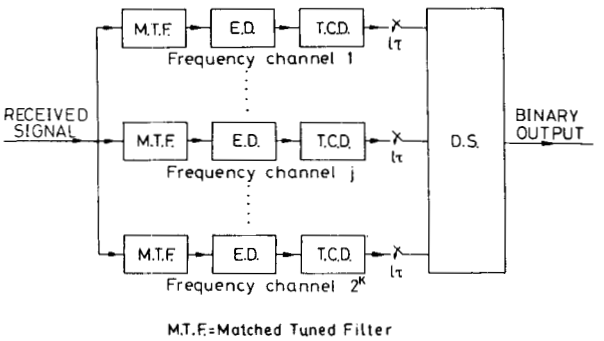

Fig. 4. 2^K-ary FSK demodulator.

$Z_0(t)$ is sampled every τ seconds in order to fill the decoding matrix and perform the majority logic decision rule every T.

B. Multicell System

The presence of cells surrounding the cell of interest (Fig. 5), and sharing the same bandwidth, originates an additional interference that degrades the performance of the isolated cell system. We can formulate the complex envelope intercell interference as

$$I_{IC}(t) = \sum_{n=1}^{N}\left[\sum_{i=-\infty}^{\infty} R_{i,n} e^{-j\theta_{i,n}} S_0(t - t_{i,n}) + \sum_{\substack{c_n=-IL \\ c_n\neq 0}}^{IR} \sum_{v=-\infty}^{\infty} R_{v,c_n} e^{-j\theta_{v,c_n}} S_{c_n}(t - t_{v,c_n})\right]$$

where N is the number of interfering cells, $R_{i,n}$ are statistically independent random variables each of which is a function of the position of mobile i in the nth cell, $\theta_{i,n}$ are statistically independent random variables and each is uniformly distributed over $[0, 2\pi]$, $\{t_{i,n}\}$ is a Poisson random point process originated by the desired channel of the interfering cell n, R_{v,c_n} and θ_{v,c_n} are identically distributed random variables as are $R_{i,n}$ and $\theta_{i,n}$, and $\{t_{v,c_n}\}$ is a Poisson random point process originated by the cth adjacent channel of the interfering cell n.

In order to characterize $R_{i,n}$ adequately, we have assumed the following.

1) The position of each mobile is a random variable uniformly distributed over the whole cell area. The positions of the different mobiles in the cell are independent random variables.

2) The mean path loss is uniform over all the service area and is distributed according to the inverse-α-power law.

3) The mean power of the received signal originated by the user of an interfering cell follows a lognormal (shadow fading) distribution.

In the presence of shadow fading, the mean received power at the base station of the cell under consideration is (see [2])

$$P_{i,n}{}^R = \gamma P \frac{r_{i,n}{}^\alpha}{(D_n{}^2 + r_{i,n}{}^2 - 2D_n r_{i,n}\cos\phi_{i,n})^{\alpha/2}}$$

where γ is a lognormal random variable, $\psi = 10 \log \gamma$ is a

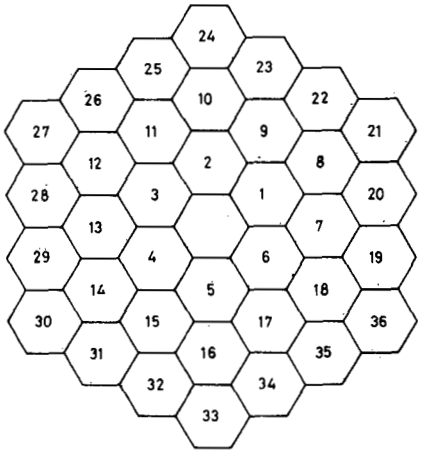

1st ring : 1st equidistant group : 1,2,3,4,5,6
2nd ring { 2nd equidistant group : 7,9,11,13,15,17
3rd equidistant group : 8,10,12,14,16,18
3rd ring { 4th equidistant group : 21,24,27,30,33,36
5th equidistant group { 19,20,22,23,25,26
28,29,31,32,34,35

Fig. 5. Layout of a multicell system.

normal random variable with mean and standard deviation given by

$$E(\psi) = 0 \text{ dB}$$

$$[E(\psi)^2]^{1/2} = \sigma_L \text{ dB},$$

$r_{i,n}$ is the distance between mobile i and its base station, D_n is the distance between the base station of the nth cell and the base station of the cell under consideration, and $\phi_{i,n}$ is the orientation angle of mobile i in the nth cell.

The complex envelope of the intercell interference signal can be written more conveniently by grouping all the intercell interference due to cells equidistant to the cell under consideration (see Fig. 5). We then obtain

$$I_{IC}(t) = \sum_{a=1}^{A} \left[\sum_{i=-\infty}^{\infty} R_{i,a} e^{-j\theta_{i,a}} S_0(t - t_{i,a}) + \sum_{\substack{c_a=-IL \\ c_a \neq 0}}^{IR} \sum_{v=-\infty}^{\infty} R_{v,c_a} e^{-j\theta_{v,c_a}} S_{c_a}(t - t_{v,c_a}) \right]$$

where A is the number of groups considered, $\{t_{i,a}\}$ is a Poisson point process of parameter $\lambda F(a)$, where $F(a)$ is the number of cells of the equidistant group a, and $\{t_{v,c_a}\}$ is a Poisson point process of parameter $\lambda F(a)$ originated by the cth adjacent channel of the equidistant group a.

IV. CALCULATION OF THE MISS AND INSERTION PROBABILITIES

As we have already stated in Section II, the calculation of the bit error probability requires the previous computation of the insertion and miss probabilities which we now outline.

A. Isolated Cell System

Referring now to Fig. 4 and considering the filtered signal $r(t)$, mentioned in Section III-A, we have that in the absence of the desired signal, the insertion probability is

$$P_I = \text{Prob}\,(|r(\tau) + n_f(\tau)| \geq C_0)$$

where C_0 is the threshold decision value. If we define r as

$$r = |r(\tau)|^2$$

then from [4] we can write

$$P_I = \int_0^{\infty} Q\left(\frac{\sqrt{x}}{\sigma_n}, \beta\right) f_r(x)\, dx$$

where $Q(\cdot, \cdot)$ is the Marcum Q function,

$$\sigma_n^2 = \tfrac{1}{2} E[|n_f(\tau)|^2]$$

$$\beta = \frac{C_0}{\sigma_n}$$

and $f_r(\cdot)$ is the probability density function of the random variable r.

Now we can calculate P_I using a Gaussian quadrature rule (GQR), which guarantees, in the area of approximate integration, the highest degree of precision

$$P_I \cong \sum_{u=1}^{N} Q\left(\frac{\sqrt{x_u}}{\sigma_n}, \beta\right) w_u.$$

The x_u are called the abscissas of the formula and the w_u the weights, so the set $\{w_u, x_u\}_{u=1}^{N}$ is called a quadrature rule corresponding to the weight function $f_r(x)$.

The lack of knowledge of $f_r(x)$, as in our case, can be bypassed by using the algorithm introduced by Golub and Welsch [5] that performs the computation of $\{w_u, x_u\}_{u=1}^{N}$ using the $2N + 1$ moments of the random variable r:

$$m_n = E(r^n); \qquad n = 0, \cdots, 2N.$$

Analogously, as we did with P_I, we can write the miss probability as

$$P_{\text{miss}} = \text{Prob}\,(|Re^{-j\theta} S_0(\tau) + r(\tau) + n_f(\tau)| < C_0).$$

Given that $RS_0(\tau)$ cos θ and $RS_0(\tau)$ sin θ are independent Gaussian random variables, we can include them in $n_x(\tau)$ and $n_y(\tau)$, respectively, and define the new variance as

$$\sigma_T^2 = \sigma_n^2 + \frac{E(R^2)}{2} |S_0(\tau)|^2.$$

Then we have

$$P_{\text{miss}} = 1 - \int_0^{\infty} Q\left(\frac{\sqrt{x}}{\sigma_T}, \frac{C_0}{\sigma_T}\right) f_r(x)\, dx.$$

The computation of the above formula can be carried out by the GQR already used to calculate P_I.

B. Multicell System

In a multicell structure we must consider as a new impairment the presence of the intercell interference signal $I_{IC}(t)$.

Then

$$P_I = \text{Prob}\,(|r(\tau) + I_{IC}(\tau) + n_f(\tau)| \geqslant C_0)$$

and

$$P_{\text{miss}} = \text{Prob}\,(|Re^{-j\theta}S_0(\tau) + r(\tau) + I_{IC}(\tau) + n_f(\tau)| < C_0).$$

Due to the large number of different contributions that are involved in the formation of $I_{IC}(t)$, we have assumed that the intercell interference is Gaussian distributed. Therefore, we can write

$$I_{IC}(t) = I_{cx}(t) + jI_{cy}(t)$$

where $I_{cx}(t)$ and $I_{cy}(t)$ are two independent Gaussian random variables with zero mean and equal variance, and

$$\sigma_I{}^2 = E[I_{cx}{}^2(t)] = E[I_{cy}{}^2(t)].$$

Once we know $\sigma_I{}^2$, we can calculate P_I and P_{miss} by the GQR given for the isolated system by substituting $\sigma_n{}^2 + \sigma_I{}^2$ for $\sigma_n{}^2$.

V. NUMERICAL RESULTS

This section contains some numerical results and curves for the design variables, $K = 8$, $L = 19$, and $W = 20$ MHz, which allow a transmission rate per user of $K/L\tau \cong 32$ kbits/s, and were chosen in [1] as optimum.

Since in this paper we deal with output signals at the reception filter whose complex envelope is of duration τ', $S_c(t) = 0\ \forall\ t \notin [0, \tau']$, $f_r(x)$ has a delta function $\delta(t)$ at the origin. Therefore we can write

$$f_r(x) = f_r(x \mid n = 0)P_{\tau'}(n = 0) + f_r(x \mid n \neq 0)P_{\tau'}(n \neq 0)$$

$$= \delta(x)P_{\tau'}(n = 0) + f_r(x \mid n = 0)P_{\tau'}(n \neq 0)$$

where $P_{\tau'}(n = 0)$ is the probability that the number of Poisson points that appear in τ' seconds is equal to zero, and

$$P_{\tau'}(n \neq 0) = 1 - P_{\tau'}(n = 0).$$

Then P_I is given by

$$P_I = \int_0^\infty Q\left(\frac{\sqrt{x}}{\sigma_n}, \beta\right) f_r(x)\,dx$$

$$= P_{\tau'}(n = 0)Q(0, \beta) + P_{\tau'}(n \neq 0) \cdot \int_0^\infty Q\left(\frac{\sqrt{x}}{\sigma_n}, \beta\right) f_r(x \mid n \neq 0)\,dx$$

$$\cong P_{\tau'}(n = 0)Q(0, \beta) + P_{\tau'}(n \neq 0) \sum_{u=1}^{N} Q\left(\frac{\sqrt{x_u}'}{\sigma_n}, \beta\right) w_u'$$

where $\{w_u', x_u'\}$ is the quadrature rule corresponding to the weight function $f_r(x \mid n \neq 0)$.

Analogously,

$$P_{\text{miss}} \cong 1 - \left[P_{\tau'}(n = 0)Q\left(0, \frac{C_0}{\sigma_T}\right) + P_{\tau'}(n \neq 0) \sum_{u=1}^{N} Q\left(\frac{\sqrt{x_u}'}{\sigma_T}, \frac{C_0}{\sigma_T}\right) w_u'\right].$$

In the GQR the moments of $f_r(x \mid n \neq 0)$ are

$$E(r^a \mid n \neq 0) = \frac{E(r^a)}{P_{\tau'}(n \neq 0)}; \qquad a \neq 0.$$

Since with GQR the convergence to the true value of the bit error probability is guaranteed, it is sufficient to check how many significant digits remain unchanged as N increases, and continue the iteration until the desired accuracy. In the numerical results of this section the convergence was obtained, at least up to the first two significant digits. P_B depends, among other factors, on β. Let β_{opt} be the value of β that minimizes P_B.

To compare the results obtained with our interference model to those given by the simplified model studied in [1], we have considered the case: $h(t) = \delta(t)$, isolated cell system, no interchannel interference, and $\beta = 2.75$ ($\cong\beta_{\text{opt}}$). Then $\tau' = \tau$ and $P_{\tau'}(n = 0) = e^{-\lambda\tau}$. Fig. 6 shows P_B versus the average signal-to-noise ratio SNR $= P/\sigma_n{}^2$ with the number of users as a parameter. In the dotted curve we have plotted the upper bound on P_B obtained in [1].

For the isolated cell system with matched receiver filters ($\tau' = 2\tau$), the value of β_{opt} depends strongly, contrary to the above simplified model, on the number of users and the average chip energy-to-one-sided power spectral noise density ratio E_c/N_0. For the β_{opt} (see Table I) calculated in the presence of the interchannel interference, we have computed P_B and plotted it in Fig. 7. The number of adjacent channels considered for this computation was $IL = IR = 4$, since by increasing this number we do not obtain a significant variation of P_B. In this case: $P_{\tau'}(n = 0) = (e^{-2\lambda\tau})^9$. For the β_{opt} values calculated in the absence of adjacent interchannel interference, we have drawn P_B in Fig. 8. Then, $P_{\tau'}(n = 0) = e^{-2\lambda\tau}$. Results shown in Fig. 6 are also valid for a synchronous model (base-to-mobile transmission) with matched filtering in the receivers. In this case the SNR value is given by

$$\text{SNR} = \frac{P}{N_0/\tau} = \frac{E_c}{N_0}.$$

For the multicell system with matched receiver filters, adjacent interchannel interference of each cell ($IL = IR = 4$), and the Gaussian approximation of the intercell interference, we have calculated P_B and plotted it in Fig. 9. The dotted curves correspond only to the first concentric ring of interference cells in the service area, and the continuous curves correspond to the first three concentric rings (see Fig. 5). By increasing this number we do not obtain appreciable variation in the values of P_B. For the multicell system $\beta_{\text{opt}} = 2.5$.

All the above curves can also be entered with the average

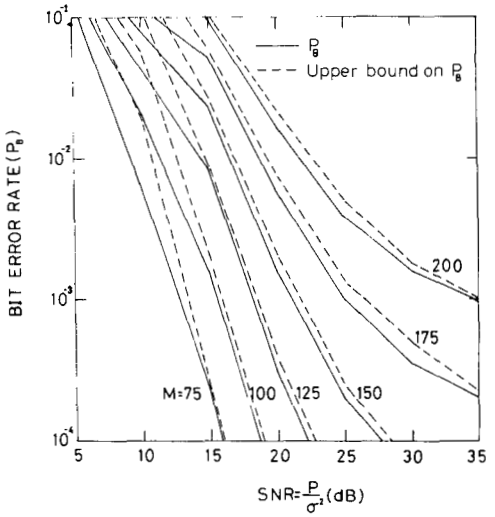

Fig. 6. Isolated cell system performance obtained with a simplified interference model.

TABLE I
β_{opt} IN AN ISOLATED CELL SYSTEM WITH MATCHED RECEIVER FILTERS AND ADJACENT INTERCHANNEL INTERFERENCE

M \ $\frac{E_c}{N_0}$	5	10	15	20	25	30
50	2.5	3.0	3.5	5.0	7.5	12.0
75	2.75	3.0	3.75	5.5	8.5	13.5
100	2.75	3.0	4.0	6.0	9.25	15.0
125	2.75	3.25	4.25	6.5	10.25	16.75
150	2.75	3.25	4.25	6.75	10.75	17.5
175	3.0	3.25	4.5	7.0	11.25	18.75
200	3.0	3.25	4.75	7.5	12.0	19.75

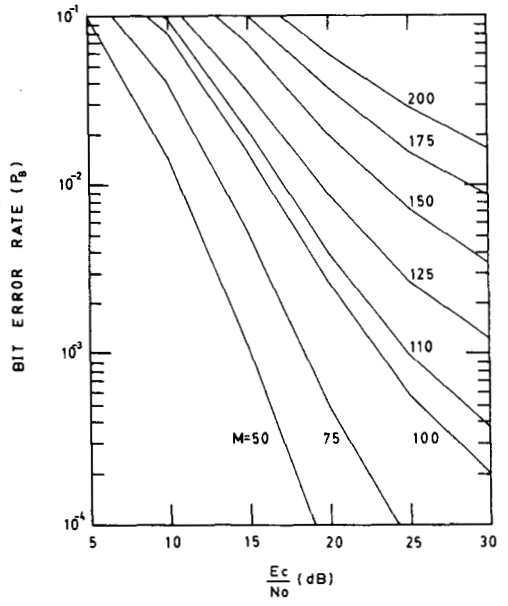

Fig. 7. Bit error probability in an isolated cell system with matched receiver filters and adjacent interchannel interference.

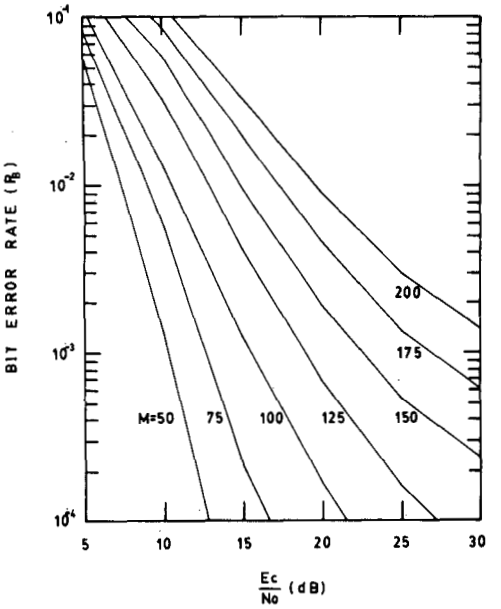

Fig. 8. Bit error probability in an isolated cell system with matched receiver filters and no adjacent interchannel interference.

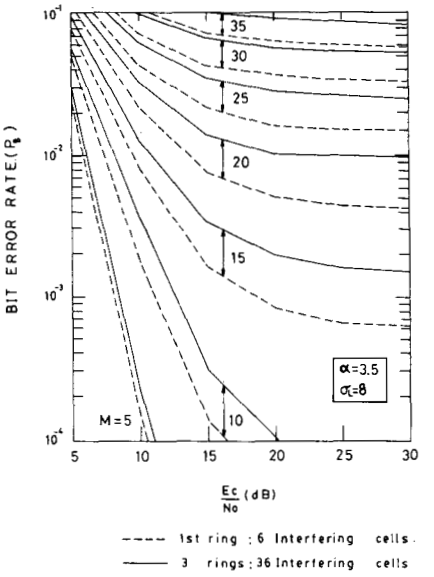

Fig. 9. Bit error probability in a multicell system with matched receiver filters and adjacent interchannel interference.

bit energy instead of the average chip energy, since

$$\left(\frac{E_b}{N_0}\right)_{dB} = \left(\frac{E_c}{N_0}\right)_{dB} + 3.75.$$

VI. CONCLUDING SUMMARY

In this paper we have presented a transmission model for an FH-MFSK digital land mobile radiotelephony system that allows us to incorporate a great number of impairments. In particular, a novel interference model has been introduced to analyze mobile-to-base communications, taking into account the interference from nonsynchronous users and adjacent channels with matched receiver filters. For intercell inter-

ference, the usual Gaussian approximation was used, but the variance calculation did take into account shadow fading. Results were obtained by integrating the conditional error probability with respect to the density function of interference using the Gaussian quadrature rule method.

Fig. 6 shows comparative results between the upper bound bit error probability obtained with a simplified chip-synchronous interference model [1] and the bit error probability obtained with our interference model with no matched filtering and no interchannel interference. Comparing Figs. 6 and 8, we observe that the number of users predicted by the synchronous model would be very close to those derived from the nonsynchronous one if the interchannel interference were not taken into account. Comparing Figs. 7 and 8, we observe that the presence of this interference introduces an important degradation. For instance, with typical SNR $= E_c/N_0 =$ 25 dB and for $P_B < 10^{-3}$, the system can accommodate up to 170 users without adjacent interchannel interference and up to 110 users with it. Comparing Figs. 7 and 9, one could conclude that intercell interference degrades the performance of FH mobile radio systems considerably, and clustering is required to control this interference.

REFERENCES

[1] D. J. Goodman, P. S. Henry, and V. K. Prabhu, "Frequency-hopped multilevel FSK for mobile radio," *Bell Syst. Tech. J.*, vol. 59, pp. 1257–1275, Sept. 1980.

[2] G. R. Cooper and R. W. Nettleton, "A spread-spectrum technique for high-capacity mobile communications," *IEEE Trans. Veh. Technol.*, vol. VT-27, Nov. 1978.

[3] A. Papoulis, *Probability, Random Variables, and Stochastic Processes*. New York: McGraw-Hill, 1965.

[4] M. Schwartz, W. R. Bennett, and S. Stein, *Communication Systems and Techniques*. New York: McGraw-Hill, 1966, pp. 399–403.

[5] G. H. Golub and J. H. Welsch, "Calculation of Gauss quadrature rules," *Math. Comput.*, vol. 23, pp. 221–230, Apr. 1969.

Comments on Electronic Techniques for Pictorial Image Reproduction

PH. W. BESSLICH

***Abstract*—The role of dither threshold matrices has not been paid much attention in a recent paper [1]. These comments highlight the useful features of the so-called Nasik pattern as a threshold matrix. It is shown that the total number of Nasik type matrices is 384. The properties of Nasik patterns are invariant to dyadic shifts. Hence, random selection of matrices and adaptive selection schemes can be devised, resulting in a minimization of texture and good rendition of details.**

Paper approved by the Editor for Communication Theory of the IEEE Communications Society for publication without oral presentation. Manuscript received July 1, 1982.

The author is with the Section of Electrical Engineering, University of Bremen, D-2800, Bremen 33, Federal Republic of Germany.

In a recent paper [1], Stoffel and Moreland surveyed techniques for reproduction of continuous-tone images by binary (black and white) printing. In one respect, the otherwise excellent paper needs some addition and a minor correction, namely, what dither threshold matrices are concerned.

Fig. 22(b) of [1] is described as a Nasik pattern. However, it seems that by mistake a wrong matrix has been taken from the cited paper by Lippel and Kurland [2]. According to [3] a certain "magic square" supposed to be invented in ancient Persia was named the Nasik pattern by A. H. Frost after a town near Bombay (India). This pattern exhibits quite a number of interesting features which makes it attractive as a dither threshold matrix. It is well known that the sum of numbers in the rows, the columns, and the nine 2 × 2 square blocks is a constant (30). Furthermore, not only the diagonals but also any row parallel to them (broken diagonal) adds to the same constant. In addition to the nine square blocks mentioned before, seven others of sum 30 may be formed if the top and bottom line as well as the right and left hand margin are thought to be connected. Finally, there are 20 patterns of (2 + 2), (2 + 1 + 1), or (1 + 1 + 1 + 1) elements, each adding up to the constant. Hence, we have a total of 52 groups of each four elements for which the sum is 30 in the matrix. It can be shown [4] that this is the maximum of four-element patterns, the values of which can add to the constant 30. There are three basic patterns possible having these remarkable properties [4]:

0	11	5	14	0	13	3	14	0	7	9	14
7	12	2	9	11	6	8	5	13	10	4	3
10	1	15	4	12	1	15	2	6	1	15	8
13	6	8	3	7	10	4	9	11	12	2	5

If the rows and the colums are periodically repeated, 16 different Nasik patterns can be obtained, each of which may be transposed and/or reflected horizontally and/or vertically. Hence, the total number of different Nasik patterns is $3 \cdot 16 \cdot 2^3 = 384$.

The use of a Nasik pattern as a dither threshold matrix provides some useful properties. For each of the 52 groups the five thresholds have the same mean. Consequently, as this applies to 52 interwoven groups, the thresholds are optimally distributed with respect to both subareas and directions.

One of the most significant advantages is that the Nasik pattern can be indefinitely repeated in any direction. Each 4 × 4 subsquare which can be marked off is of the Nasik type.

Against these advantages we must hold a small disadvantage: as the numbers 3 and 4 as well as 11 and 12 are adjacent, the resolution is slightly less than it is for the matrix given in [1, Fig. 22(b)]. However, this disadvantage is overruled by the fact that less conspicuous and objectionable artifacts result from the Nasik type matrices (Figs. 1 and 2).

In order to dissolve the artificial texture imposed by spatial concatenation of only one matrix, a random selection of dither matrices may be introduced. Fig. 3 shows the result of selecting a dither matrix for each 4 × 4 subpicture from the 384 Nasiks via a pseudorandom number. The artifacts have changed to a random pattern, similar to the one in a grainy

0090-6778/83/0600-0846$01.00